Published in final edited form as:
Int J Pharm. 2013 September 15; 454(1): 149–157. doi:10.1016/j.ijpharm.2013.07.010.

Preparation, characterization, and transport of dexamethasone-loaded polymeric nanoparticles across a human placental *in vitro* model

Hazem Ali[a], **Irina Kalashnikova**[a], **Mark Andrew White**[b], **Michael Sherman**[b], and **Erik Rytting**[a,c,d]

[a]Department of Obstetrics & Gynecology, University of Texas Medical Branch, Galveston, Texas, USA

[b]Department of Biochemistry and Molecular Biology and the Sealy Center for Structural Biology & Molecular Biophysics, University of Texas Medical Branch, Galveston, Texas, USA

[c]Center for Biomedical Engineering, University of Texas Medical Branch, Galveston, Texas, USA

[d]Department of Pharmacology & Toxicology, University of Texas Medical Branch, Galveston, Texas, USA

Abstract

The purpose of this study was to prepare dexamethasone-loaded polymeric nanoparticles and evaluate their potential for transport across human placenta. Statistical modeling and factorial design was applied to investigate the influence of process parameters on the following nanoparticle characteristics: particle size, polydispersity index, zeta potential, and drug encapsulation efficiency. Dexamethasone and nanoparticle transport was subsequently investigated using the BeWo b30 cell line, an *in vitro* model of human placental trophoblast cells, which represent the rate-limiting barrier for maternal-fetal transfer. Encapsulation efficiency and drug transport were determined using a validated high performance liquid chromatography method. Nanoparticle morphology and drug encapsulation were further characterized by cryo-transmission electron microscopy and X-ray diffraction, respectively. Nanoparticles prepared from poly(lactic-*co*-glycolic acid) were spherical, with particle sizes ranging from 140–298 nm, and encapsulation efficiency ranging from 52–89%. Nanoencapsulation enhanced the apparent permeability of dexamethasone from the maternal compartment to the fetal compartment more than 10-fold in this model. Particle size was shown to be inversely correlated with drug and nanoparticle permeability, as confirmed with fluorescently-labeled nanoparticles. These results highlight the feasibility of designing nanoparticles capable of delivering medication to the fetus, in particular, potential dexamethasone therapy for the prenatal treatment of congenital adrenal hyperplasia.

Corresponding author: Erik Rytting, Department of Obstetrics & Gynecology, University of Texas Medical Branch, 301 University Boulevard, Galveston, Texas 77555-0587, USA, Telephone: +1-409-772-2777, Fax: +1-409-747-0266, erik.rytting@utmb.edu.

The authors report no conflicts of interest.

Keywords

Dexamethasone; nanoparticles; congenital adrenal hyperplasia; BeWo cells; placenta; pregnancy

1. INTRODUCTION

Dexamethasone has been used as prenatal therapy for female fetuses diagnosed with congenital adrenal hyperplasia (CAH) (Ritzén, 2001). CAH is an inherited genetic defect, with 21-hydroxylase deficiency being the most common form. Decreased production of cortisol leads to overproduction of androgens, which causes virilization of external genitalia in affected female fetuses (Nimkarn et al., 2011). Other symptoms of this disorder include abnormal menstrual periods or even failure to menstruate, deep voice, and excessive hair growth (New, 2004).

In families with a previously affected child, antenatal prophylaxis with dexamethasone should begin before the 7^{th} week of gestation (Vos and Bruinse, 2010). Shortly thereafter, chorionic villus sampling can be used to confirm a diagnosis of CAH (New et al., 2001). Dexamethasone therapy will continue throughout the pregnancy for affected female fetuses, but the prophylaxis can be discontinued for non-affected fetuses (Nimkarn and New, 2009).

Despite its great therapeutic value to prevent neonatal abnormalities such as ambiguous genitalia, long-term prenatal administration of dexamethasone can produce unwanted side effects to the mother. These side effects include weight gain, hypertension, hyperglycemia, emotional irritability, edema, exogenous Cushing syndrome, striae with permanent scarring, and facial hair (Yankowitz and Weiner, 1995; Nimkarn and New, 2010; Merce Fernandez-Balsells et al., 2010).

A nanoparticle-based drug delivery system may represent an innovative approach to achieve prenatal dexamethasone therapy for fetal CAH while minimizing adverse effects in the mother. Polymeric nanoparticles are aqueous colloidal dispersions in the range of 50-1000 nm, the matrix of which is composed of biodegradable and biocompatible polymers. The drug can be dissolved, entrapped, encapsulated, or attached to the nanoparticle matrix (Soppimath et al., 2001). Furthermore, encapsulating drugs in polymeric nanoparticles may increase *in vivo* drug stability (Bennewitz and Saltzman, 2009).

Various polymers have been used in drug delivery research to increase therapeutic value and simultaneously minimize the associated side effects (Kreuter, 1994). The prolonged drug release offered by these polymers depends mainly on the molecular weight, the copolymer composition, and the structure of nanoparticles (Campolongo and Luo, 2009). In the past two decades, the biodegradable and biocompatible polymer poly(DL-lactide-*co*-glycolide) (PLGA) has demonstrated excellent safety profiles (Jain, 2000). PLGA has been approved by the Food and Drug Administration (FDA), and several PLGA-based products have already been introduced to the market (Ogawa et al., 1989; Okada, 1997). Therefore, PLGA has been extensively studied and has received much interest in the field of nanocarriers for drug delivery (Budhian et al., 2008; Chan et al., 2009; Dillen et al., 2006; Nafee et al., 2007; Parajó et al., 2010; Rahman et al., 2010; Song et al., 2008a; Song et al., 2008b; Zou et al., 2009).

In pharmaceutical manufacturing, quality by design (QbD) approaches have been implemented to identify the influence of critical variables—such as formulation components and process parameters—on the quality attributes of the products (Rahman et al., 2010). Many statistical designs of experiments have been adopted for optimization of the

formulation ingredients and the process parameters (Ali et al., 2010; Cun et al., 2010; Desai et al., 2008; Rahman et al., 2010). Polymeric nanoparticles can be manufactured by a modified solvent displacement method in which an organic solution of the drug and polymer is injected into an aqueous solution, followed by evaporation of the organic solvent (Beck-Broichsitter et al., 2010). The formulation ingredients—such as polymer, drug, and surfactant—can influence the physical properties of the resultant nanoparticles, including particle size, polydispersity index (PDI), and zeta potential. For instance, polydispersity resulting from the presence of microparticles can affect the quality of a nanosuspension. Therefore, optimization of nanoparticle preparation parameters can guide the production of nanoparticles with specific attributes.

Previous investigations of nanoparticles and placental transport have included studies utilizing gold nanoparticles (Myllynen et al., 2008), polystyrene nanoparticles (Wick et al., 2010; Cartwright et al., 2012), fluorescent PAMAM dendrimers (Menjoge et al., 2011), silica and titanium dioxide nanoparticles (Yamashita et al., 2011), silicon nanoparticles (Refuerzo et al., 2011), and cadmium oxide nanoparticles (Blum et al., 2012). However, none of these reports have included PLGA nanoparticles, nor have they investigated the potential for PLGA nanoparticle-mediated drug transport across the placenta.

In this work, we have undertaken the task to prepare dexamethasone-loaded PLGA nanoparticles in order to investigate their transplacental transport using the BeWo b30 cell line, an *in vitro* model of human placental trophoblast cells (Bode et al., 2006; Rytting et al., 2007). Transport of the drug across the placenta from the maternal circulation to the fetal circulation is necessary for successful fetal dexamethasone therapy. In addition, we have used a quality by design (QbD) approach to investigate the effects of formulation parameters on the physical characteristics of the drug-loaded nanoparticles. Although the preparation of dexamethasone-loaded nanoparticles has been reported previously (Gómez-Gaete et al., 2007; Kim and Martin, 2006; Lu et al., 2008; Xiang et al., 2007; Panyam et al., 2004), a full factorial design has been employed in this work to evaluate the influence of polymer, drug, and surfactant concentrations on particle size, PDI, zeta potential, and encapsulation efficiency. Encapsulation efficiency was confirmed by X-ray diffraction measurements, and particle size was confirmed by transmission electron microscopy. Nanoparticles were subsequently employed for *in vitro* transplacental transport studies to predict maternal-fetal dexamethasone transfer. Not only does this work highlight the influence of process parameters on nanoparticle properties and their transport across placental trophoblast cells *in vitro*, but it also establishes the feasibility of nanomedicine for prenatal fetal drug therapy.

2. MATERIALS AND METHODS

2.1. Materials

Acetone was purchased from Acros Organics (Fair Lawn, NJ); HPLC grade acetonitrile was purchased from Fisher Scientific (Fair Lawn, NJ); carboxylate end group 50:50 poly(D,L-lactide-*co*-glycolide) (PLGA, inherent viscosity 0.15-0.25 dL/g) was purchased from Durect Corporation (Pelham, AL, USA); coumarin-6 was purchased from Acros Organics (Fair Lawn, NJ); dexamethasone was purchased from Axxora, LLC (San Diego, CA); Dulbecco's Modified Eagle's Medium (DMEM) was purchased from Gibco® (Grand Island, NY); Dulbecco's Phosphate-Buffered Saline (1×, without calcium & magnesium) was purchased from Cellgro Mediatech, Inc. (Manassa, VA); fetal bovine serum (FBS) was purchased from Atlanta Biologicals, Inc. (Lawrenceville, GA); human placental collagen (type IV) was purchased from Sigma-Aldrich (St. Louis, MO); HPLC grade methanol was purchased from Ricca Chemical (Arlington, TX); non-essential amino acids solution was purchased from Sigma-Aldrich (St. Louis, MO); penicillin/streptomycin and L-glutamine were purchased

from Cellgro Mediatech, Inc. (Manassas, VA); sodium taurocholate was purchased from Pfaltz & Bauer, Inc. (Waterbury, CT).

2.2. Experimental design

An 18-run, three-factor, multiple-level full factorial design was applied in this study to construct second order polynomial models to describe the effect of formulation parameters on the physical properties of polymeric nanoparticles. The experimental design and the polynomial models were generated with the aid of JMP® 7 statistical software (SAS Institute Inc., Cary, NC). The following is the general formula for the models:

$$Y=A_0+A_1X_1+A_2X_2+A_3X_3+A_4X_1X_2+A_5X_2X_3+A_6X_1X_3+A_7X_1^2+A_8X_2^2+A_9X_3^2+E$$

where A_0-A_9 are the coefficients of the respective variables and their interaction terms, and E is an error term. The independent variables were dexamethasone concentration in acetone (X_1), (1–4 mg/mL), PLGA concentration in acetone (X_2), (20–60 mg/mL), and sodium taurocholate concentration in the aqueous phase (X_3), (0.5–1.0 % (w/v)). The dependent variables were Z-average particle size (Y_1), polydispersity index (PDI, Y_2), zeta potential (ζ,Y_3), and entrapment efficiency (Y_4). Results of statistical analysis were considered significant if $p<0.05$.

2.3. Preparation of Nanoparticles

Polymeric nanoparticles (Table 1) were prepared at 25°C by a modified solvent displacement method as described previously (Beck-Broichsitter et al., 2010). Briefly, PLGA and dexamethasone were dissolved in 1 mL of acetone and injected at a flow rate of 6 mL/min using a peristaltic pump (Traceable® Calibration Control Company, Friendswood, TX) into a magnetically stirred (500 rpm) aqueous phase (5 mL) consisting of purified water or an aqueous sodium taurocholate solution. After injection, the resulting colloidal suspension was continuously stirred (850 rpm) under a fume hood for 4-5 hours to allow complete evaporation of acetone. Fluorescently-labeled nanoparticles containing coumarin-6 (0.3% loading, w/w) were prepared by the same procedure mentioned above, with PLGA (20 or 40 mg/mL in acetone) and water (5 mL), only the vials were wrapped with aluminum foil for protection from light.

2.4. Measurement of particle size, size distribution, and zeta potential (ζ)

Samples were diluted to 10% with purified water and their corresponding Z-average particle size and PDI were measured by dynamic light scattering at 25°C with backscatter detection (173°) using an High Performance Particle Sizer (Malvern Instruments, Malvern, UK). The PDI describes the deviation of the measured autocorrelation function during particle size analysis from that of monodisperse spheres having the same diameter (Jores et al., 2004). Zeta potential was measured at 25°C by laser Doppler velocimetry using a Zetasizer 2000 (Malvern Instruments, Malvern, UK). Analyses were performed in triplicate unless otherwise specified.

2.5. HPLC method validation for dexamethasone analysis

Please refer to the Supplementary Data files accompanying this manuscript for details regarding validation of the high performance liquid chromatography method applied to the detection of dexamethasone in this work. Briefly, a 4.6 × 75 mm C_{18} Symmetry® analytical column (Waters, Milford, MA) with 5 μm particle size and 100 Å pore size was used with a 1 mL/min isocratic flow of mobile phase consisting of water:acetonitrile:methanol at a

50:25:25 (v:v:v) ratio. Detection of 10 μL sample injections was carried out at λ = 254 nm at 25°C.

2.6. Determination of nanoparticle entrapment efficiency

To determine the amount of dexamethasone incorporated into the nanoparticles, a 500-μL aliquot of the nanoparticle suspension was placed in the upper chamber of Vivaspin® 6 centrifugal concentrator (100 kDa molecular weight cut-off, Sartorius Stedim Biotech GmbH, Göttingen, Germany). The assembly was then centrifuged at 3000 rpm for 15 minutes at 25°C using an Eppendorf® 5810R centrifuge (Hamburg, Germany). The nanoparticles—including the encapsulated dexamethasone—remained in the upper chamber, while the aqueous filtrate contained the free, unencapsulated dexamethasone. After centrifugation, the concentration of free dexamethasone was quantified by HPLC. Encapsulation efficiency was calculated from the following equation:

$$\text{Entrapment efficiency } (\%) = \frac{\text{Mass of drug added to the nanoparticles} - \text{Mass of free drug}}{\text{Mass of drug added to the nanoparticles}} \times 100\%$$

2.7. Cryo-Transmission Electron Microscopy (cryo-TEM)

To minimize potential morphological changes during specimen preparation and imaging, the nanoparticles were vitrified as reported previously (Sherman and Weaver, 2010) on holey carbon film grids (C-flat™, Protochips, Raleigh, NC). Briefly, the aqueous nanosuspension water was applied to the holey films in a volume of ~ 2 μL, blotted with filter paper, and plunged into liquid ethane cooled in a liquid nitrogen bath. Frozen grids were stored under liquid nitrogen and transferred to a cryo-specimen 626 holder (Gatan, Inc., Pleasanton, CA) under liquid nitrogen before loading them into a JEOL 2200FS electron microscope, with a field emission gun, operating at 200 keV. Grids were maintained at near-liquid nitrogen temperature (−172 to −180°C) during imaging. Particles were imaged at 25,000× indicated microscope magnification with a 4k × 4k slow-scan CCD camera (UltraScan 895, Gatan, Inc., Pleasanton, CA) using a low-dose imaging procedure (Sherman and Weaver, 2010).

2.8. Freeze-drying

Prior to the X-ray diffraction studies, nanoparticle dispersions were frozen at −80°C. Samples were then lyophilized for 24 hours using a FreeZone 2.5L Benchtop Freeze Dry System (Labconco, Kansas City, MO) at a temperature of −50°C and a vacuum of 0.055 mbar.

2.9. X-ray diffraction measurements

The crystallinity of the dexamethasone-loaded nanoparticles was evaluated at room temperature with a DIP2030 X-ray diffractometer (Yokohama, Japan). X-ray diffraction patterns were obtained by wide-angle X-ray scattering (WAXS, 2θ=5-50°, step size = 0.04) using a MacScience DIP2030H-VLM dual 30 cm diameter imaging plate detector with an M06XHF22, 100 μm ultra-fine-focus high-brilliancy X-ray generator and RIGAKU Blue focusing multilayer optics. Data were recorded at a detector distance of 100 mm using Cu radiation (λ=1.5418 Å) at an anode voltage of 40 kV and a current of 30 mA. The freeze-dried nanoparticle samples were mounted in MiTeGen MicroRT capillaries and rotated during exposure. A blank, empty capillary exposure was used for background subtraction. The data were processed using FIT2D software (provided by Dr. Joseph Reibenspies, Texas A&M University, College Station, TX) to convert the images into plots of intensity versus 2θ.

2.10 Transport studies across BeWo cells

BeWo cells (clone b30) were obtained from Dr. Phillip Gerk (Virginia Commonwealth University). Cell culture was carried out following previously described protocols (Bode et al., 2006; Cartwright et al., 2012). Briefly, the cells were cultured in DMEM with 10% FBS supplemented with penicillin/streptomycin, L-glutamine and nonessential amino acids and maintained at 37°C, 5% CO_2, and 95% relative humidity. Cells were passed every 5-7 days; cell passage numbers 36-40 were used in this study. Prior to transport experiments, cells were seeded at a density of 100,000 cells/cm^2 onto polycarbonate Transwell® inserts (pore size 3.0 μm, 1.12 cm^2 growth area, apical volume 0.5 mL, basolateral volume 1.5 mL, Corning Inc., Corning, NY) coated with human placental collagen. The cell culture medium was changed daily until the cell monolayers reached confluence (after 5-7 days). The formation of tight junctions for barrier integrity and the presence of a single monolayer on the filters were confirmed by measuring the transepithelial electrical resistance (TEER) using an EndOhm-12 apparatus (World Precision Instruments, Sarasota, FL). The TEER was measured in growth media (DMEM) at room temperature and calculated as the measured resistance minus the resistance of an empty Transwell® insert (blank without cells). Only the Transwell® inserts with cell monolayers displaying TEER values of at least 30±2 Ω·cm^2 were used in the nanoparticle transport studies (Mørck et al., 2010), and values were as high as 61±2 Ω·cm^2. The uncertainty of ±2 Ω·cm^2 for each individual measurement reflects the instrument's variation between successive resistance measurements of the same sample. Following the TEER measurements, the cells were equilibrated in DMEM for 30–45 min at 37°C.

At time zero, nanoparticle dispersions were vortexed in transport medium (DMEM) and added to the apical chamber. The transport experiment was carried out under cell culture conditions (37°C, 5% CO_2, 95% humidity) with constant stirring. At the specified time points, 100 μL samples were removed from the basolateral chamber and replaced with 100 μL of fresh transport medium. Experiments were carried out in quadruplicate in parallel with transport studies across blank Transwell® inserts with no cells (for determination of apparent permeability values, as described below). The collected samples were analyzed by HPLC for determination of dexamethasone concentrations as described in the Supplementary Data files accompanying this manuscript. For the transport experiments with the coumarin-6-loaded nanoparticles, the sample and replacement volumes were 200 μL, and fluorescence detection was carried out using an FLx800 microplate reader (BioTek, Winooski, VT) with λ_{ex} = 485 nm and λ_{em} = 528 nm.

At each time point $t = t_n$, the mass transported (ΔQ_n) was determined and corrected for the mass removed during the previous sampling periods using the following equation:

$$\Delta Q_n = C_n \cdot V_w + \sum_{j=1}^{n-1} V_s \cdot C_j$$

where C_n is the concentration measured at time t_n, V_w is the volume of the well sampled (in this case, 1.5 mL from the basolateral chamber), V_s is the sampling volume (in this case, 100 μL for the dexamethasone transport studies and 200 μL for the transport of coumarin-6-loaded nanoparticles), and the term $\sum_{j=1}^{n-1} V_s.C_j$ represents the correction for the cumulative mass removed by sampling during all the sampling periods prior to t_n (from $t = t_1$ until $t = t_{n-1}$). Data were converted to permeability values (P) with the following equation:

$$P = \frac{\Delta Q/\Delta t}{A \cdot C_0}$$

where $\Delta Q/\Delta t$ is the mass flux, A is the surface area of the layer, and C_0 is the initial concentration on the donor side.

The apparent permeability (P_e) across the cell monolayer alone was calculated from the permeability across blank Transwell® filter membranes without cells (P_m) and the permeability across Transwell® inserts containing cells (P_t) with the following equation (Poulsen et al., 2009):

$$P_e = \frac{1}{\left(\frac{1}{P_t} - \frac{1}{P_m}\right)}$$

In order to ensure the integrity of the BeWo cell monolayers, the apparent permeability of the paracellular tracer Lucifer yellow (Lucifer yellow CH lithium salt from Biotium, Inc., Hayward, CA) was investigated on days 3-6 post-seeding. The cells were cultured in RPMI 1640 (Mediatech, Manassas, VA) with supplements and 10% FBS. Immediately prior to these transport studies, TEER measurements were recorded and then the cells were washed with warm (37°C) Hank's Balanced Salt Solution (HBSS, Mediatech). Fresh warm HBSS was then added to the cells for equilibration in the incubator for 30-45 minutes. The HBSS was removed, the basolateral chamber was replaced with 1.5 mL of HBSS + 1% dimethyl sulfoxide (DMSO, Sigma), and then at time zero, 0.5 mL of 60 μM Lucifer yellow in HBSS + 1% DMSO was added to the apical chamber. The transport studies were performed in quadruplicate with duplicate blanks and samples were analyzed by fluorescence detection (λ_{ex} = 420 nm, λ_{em} = 528 nm). Different cell monolayers were used on each post-seeding day, i.e., cells were not re-used for the subsequent days' experiments. Apparent permeability (P_e) was calculated as described above.

2.11. Statistical analysis

Data collected in this study were analyzed by one-way analysis of variance (ANOVA) followed by Tukey-Kramer multiple comparison tests using NCSS statistical software (Kaysville, UT). Results of the statistical analysis were considered significant if their corresponding *p*-values were less than 0.05.

3. RESULTS AND DISCUSSION

3.1. Experimental design

An 18-run, three-factor, multiple-level full factorial design was utilized in this study to correlate the effects of dexamethasone concentration in acetone ([DEX], mg/mL, X_1), PLGA concentration in acetone ([PLGA], mg/mL, X_2), and sodium taurocholate concentration ([ST], % w/v, X_3) on the average particle size (Y_1, nm), PDI (Y_2, unitless), zeta potential (ζ,Y_3, mV), and encapsulation efficiency (Y_4, %). Table 1 shows the design variables and the observed responses. Model analysis showed that the polynomial quadratic model was statistically significant for Y_1, Y_3, and Y_4 ($p < 0.0001$, $p < 0.05$, and $p < 0.01$, respectively). The equations constructed for these responses are as follows:

$$\text{Particle Size} = 100.3 + 3.1 \cdot [\text{PLGA}]$$

$$\text{Zeta potential} = -60.0 - 7.0 \cdot [\text{ST}]$$

$$\text{Encapsulation efficiency} = 40.1 + 5.5 \cdot [\text{DEX}] + 4.5 \cdot [\text{DEX}]^2 + 0.02 \cdot [\text{PLGA}]^2$$

The contour plots in Figure 1 describe these responses graphically. Both these plots and the equations above show the linear effect of polymer concentration on particle size, the linear effect of sodium taurocholate concentration on zeta potential, and the quadratic effect of both dexamethasone concentration and polymer concentration on the encapsulation efficiency. There was no significant model effect on PDI (Y_2, $p = 0.784$). Nevertheless, most formulations demonstrated monomodal particle size distribution (Dong et al., 2009), with all nanoparticles prepared with PLGA concentrations below 60 mg/mL having PDI values below 0.4. For this reason, nanoparticles prepared with 60 mg/mL PLGA were not investigated further.

As demonstrated in both Table 1 and Figure 1, the particle size increased with increasing concentrations of PLGA. This phenomenon has been observed previously and attributed to the increasing number of polymer chains per unit volume of organic solvent dispersed during the nanoprecipitation event (Galindo-Rodriguez et al., 2004). Although solvent viscosity itself was not a variable in the present factorial design, it is a property that can be affected by polymer concentration. A more detailed discussion concerning the influence of solvent viscosity on particle size for nanoparticles prepared by the solvent displacement method has been presented previously and will not be repeated here (see Beck-Broichsitter et al., 2010). The decreased zeta potential values observed upon the increased concentration of sodium taurocholate in the aqueous phase can be expected due to the negative charge imparted by taurocholate to the nanoparticle surfaces.

The increased encapsulation efficiency with increased theoretical drug loading may reflect the limited aqueous solubility of dexamethasone; i.e., a limited (but constant) amount of drug is soluble in the aqueous phase and is therefore not encapsulated in the polymeric nanoparticle matrix. However, as more drug is added to the formulation, a smaller relative percentage of the drug is lost to aqueous dissolution and a higher percentage remains in the nanoparticles. Gómez-Gaete et al. (2007) observed a similar trend when preparing dexamethasone-loaded PLGA nanoparticles by the emulsion/solvent evaporation method. Drug loading increased as a function of the mass of dexamethasone added, up to a maximum at 10 mg of drug added to 100 mg of polymer. These authors compared the effects of various solvents and lactide composition on drug loading and suggested that competition between crystallization forces and the saturation of the polymer matrix by the drug may affect the drug encapsulation process. Panyam et al. (2004) also prepared dexamethasone-loaded PLGA nanoparticles by the emulsion/solvent evaporation method and had similarly pointed out the importance of the solid-state solubility of the drug in the polymer. They investigated the influence of polymer properties such as molecular weight, lactide composition, and ester versus acid end groups; they observed higher drug loading values at higher phase separation concentrations of dexamethasone in the various polymers.

In this work, dexamethasone-loaded nanoparticles were prepared by a solvent displacement method, rather than by the emulsion/solvent evaporation method which had been employed by both Panyam et al. (2004) and Gómez-Gaete et al. (2007). It is interesting to note that the encapsulation efficiency values obtained for nanoparticles prepared by solvent displacement

were greater than 50% (see Table 1), whereas the encapsulation efficiency of dexamethasone nanoparticles in the aforementioned reports did not exceed 50%.

Besides drug loading, another important parameter to consider in the design of nanoparticles for potential transplacental drug delivery is the particle size. As will be seen below, smaller particles promoted increased nanoparticle and drug permeability across BeWo cells. Therefore, in terms of utilizing the information obtained from the experimental design, optimal nanoparticles with high encapsulation efficiency and small particle size could be obtained with low polymer concentration and increased drug loading. Because the polymer concentration is a variable which affects both particle size and encapsulation efficiency, it would seem that some type of balance must be reached in order to optimize the process. Nevertheless, it should be noted that the equation above represents the contribution of polymer concentration to encapsulation efficiency with a coefficient of only 0.02, which is relatively minor compared to the influence of the concentration of dexamethasone in the same equation (see also Figure 1C).

3.2 HPLC method validation

Please refer to the Supplementary Data files accompanying this manuscript for details regarding the HPLC method validation results.

3.3. X-ray diffraction studies

As the nanoparticle matrix has a limited capacity for drug loading, there is the possibility that attempts to incorporate excess amounts of drug could lead to drug crystallization during the formulation process. Wide-angle X-ray diffraction was utilized to study the physical state of dexamethasone upon nanoencapsulation. X-ray diffraction is an established technique that has been used to characterize solid dispersions and evaluate the degree of crystallization and polymorphism of drugs. Formulation #1 from Table 1 was freeze dried and analyzed by X-ray diffraction as described in the experimental section. The X-ray diffraction pattern for bulk dexamethasone revealed major peaks at 2θ = 6.1, 9.1, 10.9, 12.86, 14.66, 15.4, and 17.02 (see Figure 2). PLGA has a characteristic broad peak at 2θ = 10–25°. Bulk sodium taurocholate, however, revealed major peaks at 7.2, 8.3, 11.9, 13.3, 14.4, 15.7, 20.6, 29.9, and 44.3°. Freeze-dried dispersions of unloaded as well as dexamethasone-loaded nanoparticles displayed only the PLGA-(2θ = 10–25°) and sodium taurocholate-derived peaks (2θ = 29.9, 44.3°). Absence of the peaks distinctive to the dexamethasone diffraction pattern suggested that it was in an amorphous state and molecularly dispersed in the partially crystalline PLGA. The physical mixture comprised of dexamethasone, PLGA, and sodium taurocholate, on the other hand, revealed the distinct peaks seen with bulk dexamethasone (2θ = 6.1, 9.1, 10.9, 12.86, 14.66, 15.4, and 17.02), indicating the presence of dexamethasone in crystalline form (Figure 2). This was confirmed by cryo-TEM, as described in the following section. Both Panyam et al. (2004) and Gómez-Gaete et al. (2007) had similarly confirmed encapsulation of dexamethasone in PLGA nanoparticles by means of X-ray diffraction.

3.4. Cryo-transmission electron microscopy (cryo-TEM)

Cryo-TEM allows for preservation of the native state of a sample by extremely rapid freezing of suspensions by so-called water vitrification (Sherman and Weaver, 2010). In this process, the fast cooling rates (> 10^5–10^6 °C/second) do not allow the water to crystallize. The water hardens like glass, leaving the specimens embedded in the solid matrix of a frozen buffer to maintain the native conformations of biological macromolecules (Lepault et al., 1983). Cryo-TEM images were collected to investigate the morphology of the dexamethasone-loaded nanoparticles. As shown in the representative image (Figure 3), the nanoparticles were of spherical shape. No dexamethasone crystals were visible, which

confirmed the observations from the X-ray diffraction analysis. The size of the nanoparticles was measured using DigitalMicrograph software (Gatan, Inc., Pleasanton, CA). The particle size data obtained with this software were in fair agreement with the particle size data obtained by dynamic light scattering that were reported in Table 1.

3.4. Transport studies across BeWo cells

The BeWo b30 human placental choriocarcinoma cell line is considered an established model of the human placental barrier (Ampasavate et al., 2002). When the cells are grown on permeable inserts, they form polarized monolayers useful for studying transplacental transport (Bode et al., 2006). The integrity of the BeWo cell monolayers on days 3-6 post-seeding was investigated by daily TEER measurements in conjunction with transport studies involving the paracellular tracer Lucifer yellow (Hidalgo et al., 1989). Figure 4 shows that by day 5 post-seeding, the apparent permeability of Lucifer yellow had reached a minimal plateau, and the TEER values were in the previously reported desirable range (Mørck et al., 2010). This means that by day 5 post-seeding, the cells had formed tight junctions which limited passive permeation.

Table 2 shows that when dexamethasone is formulated in PLGA nanoparticles, the apparent permeability (P_e) of dexamethasone from the apical (maternal) side of the BeWo cells to the basolateral (fetal) side increased by an order of magnitude compared to the permeability of dexamethasone alone. This increase was statistically significant ($p < 0.0001$). The enhanced permeability resulting from the encapsulation of dexamethasone into the biocompatible PLGA nanoparticles may be due to differences in protein binding and altered interactions with efflux transporters in the apical membrane of trophoblast cells; additional studies are underway to elucidate these possibilities.

Just as we had investigated the influence of variables such as polymer, sodium taurocholate, and drug concentrations on the physicochemical properties of the nanoparticles themselves (see Table 1 and Figure 1), we also studied the influence of sodium taurocholate and particle size on the apparent permeability of dexamethasone across BeWo cell monolayers upon administration of dexamethasone-loaded nanoparticles to the apical chamber. Table 3 shows that the presence of sodium taurocholate substantially increases the permeability of dexamethasone, even without nanoparticles. The P_e of dexamethasone alone in the presence of sodium taurocholate was more than 5-times higher than the P_e of dexamethasone alone without sodium taurocholate ($p < 0.01$). This is most likely due to the surfactant properties of sodium taurocholate and its effect on the cell monolayer (Lin et al., 2007). This trend is also seen upon comparison of dexamethasone permeability data for the dexamethasone-loaded nanoparticle formulations. With particle size held relatively constant (near 150 nm), Table 3 demonstrates that P_e increased with the increase in the sodium taurocholate concentration employed during nanoparticle preparation. The P_e of dexamethasone for the nanoparticles prepared in 1.0% (w/v) sodium taurocholate was significantly higher ($p < 0.01$) than the permeability of dexamethasone for the other formulations.

The data in Table 4 compares the influence of nanoparticle size on dexamethasone transport across BeWo cell monolayers. With the sodium taurocholate concentration held constant, the P_e of dexamethasone was 25% higher for the smaller particles (146 nm) than the P_e for the larger particles (232 nm). Previous reports have demonstrated the influence of particle size on the transplacental transport of polystyrene nanoparticles (Cartwright et al., 2012; Wick et al., 2010). Although the transplacental transport of PLGA nanoparticles has not been published previously, we expected that the increased permeability of dexamethasone resulting from the application of the smaller drug-loaded nanoparticles might be due to increased permeability of the nanocarriers themselves. In order to investigate this possibility, fluorescent PLGA nanoparticles containing coumarin-6 (but not containing any

dexamethasone) were prepared at two particle sizes (145 nm and 196 nm). These nanoparticles were prepared in purified water without sodium taurocholate in order to eliminate any surfactant effects on this investigation of size-dependent transport. Fluorescence detection was used to track the accumulation of these nanoparticles in the basolateral (fetal) chamber during the transport studies, and particle size measurements were made at the beginning and at the end of transport studies. The average particle size of the nanoparticles in the basolateral chamber (i.e., the size of nanoparticles which had crossed the cell monolayers) was not significantly different from the particle size determined in the apical chamber at the start of the experiment. Figure 5 shows that the P_e of the 145-nm fluorescent nanocarriers was twice as high as the P_e of the 196-nm particles ($p < 0.05$). Therefore, particle size was shown to influence the nanoparticle-mediated delivery of dexamethasone across this *in vitro* model of human placental trophoblast.

4. CONCLUSIONS

Dexamethasone-loaded PLGA nanoparticles were successfully prepared by a modified solvent displacement method. Results of the factorial design indicated the influence of process parameters on the particle properties. The influence of these nanoparticle properties, in turn, upon the transplacental permeability of dexamethasone was investigated and compared to the permeability of dexamethasone alone across BeWo b30 cell monolayers, an *in vitro* model of human placental trophoblast cells. Nanoencapsulation enhanced the apparent permeability of dexamethasone from the maternal compartment to the fetal compartment in this model, and particle size was shown to be inversely correlated with drug and nanoparticle permeability. To the best of our knowledge, this is the first report regarding the transplacental transport of PLGA nanoparticles, and our results highlight the feasibility of designing nanoparticles capable of delivering medication to the fetus. In particular, these results may lead to promising advancements in dexamethasone therapy for the prenatal treatment of congenital adrenal hyperplasia. The results presented in this manuscript represent the first steps in the development of nanoparticles capable of delivering drugs across the placenta for fetal drug therapy. Additional *in vivo* studies are needed to investigate the tissue distribution of both the nanoparticles and the drug.

Supplementary Material

Refer to Web version on PubMed Central for supplementary material.

Acknowledgments

The authors are grateful to Dr. Joseph Reibenspies (Texas A&M University, College Station, TX) for providing the FIT2D software for X-ray diffraction analysis and to Sanaalarab Al Enazy for her assistance with the graphical abstract. E.R. is supported by a research career development award (K12HD052023: Building Interdisciplinary Research Careers in Women's Health Program, BIRCWH) from the National Institute of Allergy and Infectious Diseases (NIAID), the NICHD, and the Office of the Director (OD), National Institutes of Health (NIH). The content is solely the responsibility of the authors and does not necessarily represent the official views of the NIAID, NICHD, OD, or the NIH.

REFERENCES

Ali H, Shirode AB, Sylvester PW, Nazzal S. Preparation and in vitro antiproliferative effect of tocotrienol loaded lipid nanoparticles. Colloids and Surfaces A: Physicochem. Eng. Aspects. 2010; 353:43–51.

Ampasavate C, Chandorkar GA, Vande Velde DG, Stobaugh JF, Audus KL. Transport and metabolism of opioid peptides across BeWo cells, an in vitro model of the placental barrier. Int. J. Pharm. 2002; 233:85–98. [PubMed: 11897413]

Beck-Broichsitter M, Rytting E, Lebhardt T, Wang X, Kissel T. Preparation of nanoparticles by solvent displacement for drug delivery: a shift in the “ouzo region” upon drug loading. Eur. J. Pharm. Sci. 2010; 41:244–253. [PubMed: 20600881]

Bennewitz MF, Saltzman WM. Nanotechnology for delivery of drugs to the brain for epilepsy. Neurotherapeutics. 2009; 6:323–336. [PubMed: 19332327]

Blum JL, Xiong JQ, Hoffman C, Zelikoff JT. Cadmium associated with inhaled cadmium oxide nanoparticles impacts fetal and neonatal development and growth. Toxicol. Sci. 2012; 126:478–486. [PubMed: 22240978]

Bode CJ, Jin H, Rytting E, Silverstein PS, Young AM, Audus KL. In vitro models for studying trophoblast transcellular transport. Methods Mol. Med. 2006; 122:225–239. [PubMed: 16511984]

Budhian A, Siegel SJ, Winey KI. Controlling the in vitro release profiles for a system of haloperidol-loaded PLGA nanoparticles. Int. J. Pharm. 2008; 346:151–159. [PubMed: 17681683]

Cartwright L, Poulsen MS, Nielsen HM, Pojana G, Knudsen LE, Saunders M, Rytting E. In vitro placental model optimization for nanoparticle transport studies. Int. J. Nanomed. 2012; 7:497–510.

Campolongo MJ, Luo D. Drug delivery: Old polymer learns new tracts. Nat. Mater. 2009; 8:447–448. [PubMed: 19458640]

Chan JM, Zhang L, Yuet KP, Liao G, Rhee JW, Langer R, Farokhzad OC. PLGA-lecithin-PEG core-shell nanoparticles for controlled drug delivery. Biomaterials. 2009; 30:1627–1634. [PubMed: 19111339]

Cun D, Jensen DK, Maltesen MJ, Bunker M, Whiteside P, Scurr D, Foged C, Nielsen HM. High loading efficiency and sustained release of siRNA encapsulated in PLGA nanoparticles: Quality by design optimization and characterization. Eur. J. Pharm. Biopharm. 2011; 77(1):26–35. [PubMed: 21093589]

Desai KG, Mallery SR, Schwendeman SP. Effect of formulation parameters on 2-methoxyestradiol release from injectable cylindrical poly(DL-lactide-co-glycolide) implants. Eur. J. Pharm. Biopharm. 2008; 70:187–198. [PubMed: 18472254]

Dillen K, Vandervoort J, Van den Mooter G, Ludwig A. Evaluation of ciprofloxacin-loaded Eudragit RS100 or RL100/PLGA nanoparticles. Int, J. Pharm. 2006; 314:72–82. [PubMed: 16600538]

Dong X, Mattingly CA, Tseng M, Cho M, Adams VR, Mumper RJ. Development of new lipid-based paclitaxel nanoparticles using sequential simplex optimization. Eur. J. Pharm. Biopharm. 2009; 72:9–17. [PubMed: 19111929]

Galindo-Rodriguez S, Allémann E, Fessi H, Doelker E. Physicochemical parameters associated with nanoparticle formation in the salting-out, emulsification-diffusion, and nanoprecipitation methods. Pharm. Res. 2004; 21:1428–1439. [PubMed: 15359578]

Gómez-Gaete C, Tsapis N, Besnard M, Bochot A, Fattal E. Encapsulation of dexamethasone into biodegradable polymeric nanoparticles. Int. J. Pharm. 2007; 331:153–159. [PubMed: 17157461]

Hidalgo IJ, Raub TJ, Borchardt RT. Characterization of the human colon carcinoma cell line (Caco-2) as a model system for intestinal epithelial permeability. Gastroenterology. 1989; 96:736–749. [PubMed: 2914637]

Jain RA. The manufacturing techniques of various drug loaded biodegradable poly(lactide-co-glycolide) (PLGA) devices. Biomaterials. 2000; 21:2475–2490. [PubMed: 11055295]

Jores K, Mehnert W, Drechsler M, Bunjes H, Johann C, Mader K. Investigations on the structure of solid lipid nanoparticles (SLN) and oil-loaded solid lipid nanoparticles by photon correlation spectroscopy, field-flow fractionation and transmission electron microscopy. J. Control. Release. 2004; 95:217–227. [PubMed: 14980770]

Kim DH, Martin DC. Sustained release of dexamethasone from hydrophilic matrices using PLGA nanoparticles for neural drug delivery. Biomaterials. 2006; 27:3031–3037. [PubMed: 16443270]

Kreuter J. Drug targeting with nanoparticles. Eur. J. Drug Metab. Pharmacokinet. 1994; 19:253–256. [PubMed: 7867668]

Lepault J, Booy FP, Dubochet J. Electron microscopy of frozen biological suspensions. J. Microsc. 1983; 129:89–102. [PubMed: 6186816]

Lin H, Gebhardt M, Bian S, Kwon KA, Shim CK, Chung SJ, Kim DD. Enhancing effect of surfactants on fexofenadine.HCl transport across the human nasal epithelial cell monolayer. Int. J. Pharm. 2007; 330:23–31. [PubMed: 16997520]

Lu X, Howard MD, Mazik M, Eldridge J, Rinehart JJ, Jay M, Leggas M. Nanoparticles containing anti-inflammatory agents as chemotherapy adjuvants: optimization and in vitro characterization. AAPS J. 2008; 10:133–140. [PubMed: 18446513]

Menjoge AR, Rinderknecht AL, Navath RS, Faridnia M, Kim CJ, Romero R, Miller RK, Kannan RM. Transfer of PAMAM dendrimers across human placenta: prospects of its use as drug carrier during pregnancy. J. Control. Release. 2011; 150:326–338. [PubMed: 21129423]

Mercè Fernández-Balsells M, Muthusamy K, Smushkin G, Lampropulos JF, Elmain MB, Abu Elnour NO, Elamin KB, Agrwal N, Gallegos-Orozco JF, Lane MA, Erwin PJ, Montori VM, Murad MH. Prenatal dexamethasone use for the prevention of virilization in pregnancies at risk for classical congenital adrenal hyperplasia because of 21-hydroxylase (CYP21A2) deficiency: a systematic review and meta-analyses. Clin. Endocrinol. (Oxf). 2010; 73:436–444. [PubMed: 20550539]

Mørck TJ, Sorda G, Bechi N, Rasmussen BS, Nielsen JB, Ietta F, Rytting E, Mathiesen L, Paulesu L, Knudsen LE. Placental transport and in vitro effects of Bisphenol A. Repro. Tox. 2010; 30:131–137.

Myllynen PK, Loughran MJ, Howard CV, Sormunen R, Walsh AA, Vähäkangas KH. Kinetics of gold nanoparticles in the human placenta. Repro. Tox. 2008; 26:130–137.

Nafee N, Taetz S, Schneider M, Schaefer UF, Lehr CM. Chitosan-coated PLGA nanoparticles for DNA/RNA delivery: effect of the formulation parameters on complexation and transfection of antisense oligonucleotides. Nanomedicine. 2007; 3:173–183. [PubMed: 17692575]

New MI. An update of congenital adrenal hyperplasia. Ann. N. Y. Acad. Sci. 2004; 1038:14–43. [PubMed: 15838095]

New MI, Carlson A, Obeid J, Marshall I, Cabrera MS, Goseco A, Lin-Su K, Putnam AS, Wei JQ, Wilson RC. Prenatal diagnosis for congenital adrenal hyperplasia in 532 pregnancies. J. Clin. Endocrinol. Metab. 2001; 86:5651–5657. [PubMed: 11739415]

Nimkarn S, Lin-Su K, New MI. Steroid 21 hydroxylase deficiency congenital adrenal hyperplasia. Pediatr. Clin. N. Am. 2011; 58:1281–1300.

Nimkarn S, New MI. Prenatal diagnosis and treatment of congenital adrenal hyperplasia due to 21-hydroxylase deficiency. Mol. Cell. Endocrinol. 2009; 300:192–196. [PubMed: 19101608]

Nimkarn S, New MI. Congenital adrenal hyperplasia due to 21-hydroxylase deficiency: a paradigm for prenatal diagnosis and treatment. Ann. N. Y. Acad. Sci. 2010; 1192:5–11. [PubMed: 20392211]

Ogawa Y, Okada H, Heya T, Shimamoto T. Controlled release of LHRH agonist, leuprolide acetate, from microcapsules: serum drug level profiles and pharmacological effects in animals. J. Pharm. Pharmacol. 1989; 41:439–444. [PubMed: 2570847]

Okada H. One- and three-month release injectable microspheres of the LH-RH superagonist leuprorelin acetate. Adv. Drug Deliv. Rev. 1997; 28:43–70. [PubMed: 10837564]

Panyam J, Williams D, Dash A, Leslie-Pelecky D, Labhasetwar V. Solid-state solubility influences encapsulation and release of hydrophobic drugs from PLGA/PLA nanoparticles. J. Pharm. Sci. 2004; 93:1804–1814. [PubMed: 15176068]

Parajó Y, d'Angelo I, Horváth A, Vantus T, György K, Welle A, Garcia-Fuentes M, Alonso MJ. PLGA:poloxamer blend micro- and nanoparticles as controlled release systems for synthetic proangiogenic factors. Eur. J. Pharm. Sci. 2010; 41:644–649. [PubMed: 20869438]

Poulsen MS, Rytting E, Mose T, Knudsen LE. Modeling placental transport: Correlation of in vitro BeWo cell permeability and ex vivo human placental perfusion. Tox. in Vitro. 2009; 23:1380–1386.

Rahman Z, Zidan AS, Habib MJ, Khan MA. Understanding the quality of protein loaded PLGA nanoparticles variability by Plackett-Burman design. Int. J. Pharm. 2010; 389:186–194. [PubMed: 20038446]

Refuerzo JS, Godin B, Bishop K, Srinivasan S, Shah SK, Amra S, Ramin SM, Ferrari M. Size of the nanovectors determines the transplacental passage in pregnancy: study in rats. Am. J. Obstet. Gynecol. 2011; 204:546.e5–e9. [PubMed: 21481834]

Ritzén EM. Prenatal dexamethasone treatment of fetuses at risk for congenital adrenal hyperplasia: benefits and concerns. Semin. Neonatol. 2001; 6:357–362. [PubMed: 11972437]

Rytting E, Bryan J, Southard M, Audus KL. Low-affinity uptake of the fluorescent organic cation 4-(4-(dimethylamino)styryl)-N-methylpyridinium iodide (4-Di-1-ASP) in BeWo cells. Biochem. Pharmacol. 2007; 73:891–900. [PubMed: 17174940]

Sherman MB, Weaver SC. Structure of the Recombinant Alphavirus Western Equine Encephalitis Virus Revealed by Cryoelectron Microscopy. J. Virol. 2010; 84:9775–9782. [PubMed: 20631130]

Song X, Zhao Y, Hou S, Xu F, Zhao R, He J, Cai Z, Li Y, Chen Q. Dual agents loaded PLGA nanoparticles: systematic study of particle size and drug entrapment efficiency. Eur. J. Pharm. Biopharm. 2008a; 69:445–453. [PubMed: 18374554]

Song X, Zhao Y, Wu W, Bi Y, Cai Z, Chen Q, Li Y, Hou S. PLGA nanoparticles simultaneously loaded with vincristine sulfate and verapamil hydrochloride: systematic study of particle size and drug entrapment efficiency. Int. J. Pharm. 2008b; 350:320–329. [PubMed: 17913411]

Soppimath KS, Aminabhavi TM, Kulkarni AR, Rudzinski WE. Biodegradable polymeric nanoparticles as drug delivery devices. J. Control. Release. 2001; 70:1–20. [PubMed: 11166403]

Vos AA, Bruinse HW. Congenital adrenal hyperplasia: do the benefits of prenatal treatment defeat the risks? Obstet. Gynecol. Surv. 2010; 65:196–205. [PubMed: 20214835]

Wick P, Malek A, Manser P, Meili D, Maeder-Althaus X, Diener L, Diener PA, Zisch A, Krug HF, von Mandach U. Barrier capacity of human placenta for nanosized materials. Environ. Health Perspect. 2010; 118:432–436. [PubMed: 20064770]

Xiang QY, Wang MT, Chen F, Gong T, Jian YL, Zhang ZR, Huang Y. Lung-targeting delivery of dexamethasone acetate loaded solid lipid nanoparticles. Arch. Pharm. Res. 2007; 30:519–525. [PubMed: 17489370]

Yamashita K, Yoshioka Y, Higashisaka K, Mimura K, Morishita Y, Nozaki M, Yoshida T, Ogura T, Nabeshi H, Nagano K, Abe Y, Kamada H, Monobe Y, Imazawa T, Aoshima H, Shishido K, Kawai Y, Mayumi T, Tsunoda S-I, Itoh N, Yoshikawa T, Yanagihara I, Saito S, Tsutsumi Y. Silica and titanium dioxide nanoparticles cause pregnancy complications in mice. Nat. Nanotechnol. 2011; 6:321–328. [PubMed: 21460826]

Yankowitz J, Weiner C. Medical fetal therapy. Baillieres Clin. Obstet. Gynaecol. 1995; 9:553–570. [PubMed: 8846556]

Zou W, Liu C, Chen Z, Zhang N. Studies on bioadhesive PLGA nanoparticles: A promising gene delivery system for efficient gene therapy to lung cancer. Int. J. Pharm. 2009; 370:187–195. [PubMed: 19073241]

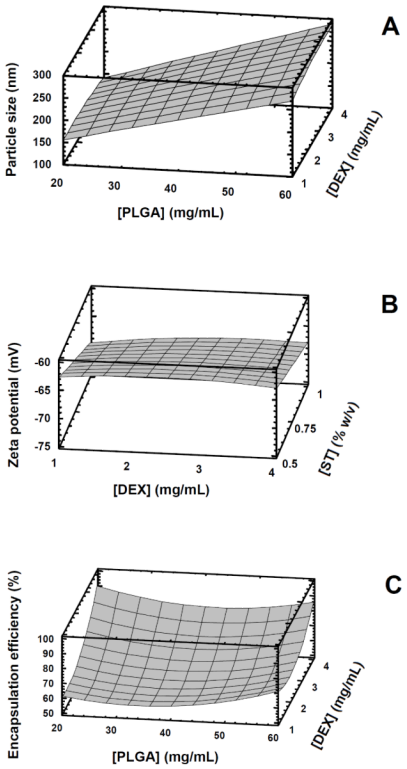

Figure 1.

Response surface plots showing the effects of the following parameters on the properties of drug-loaded nanoparticles: **A**. Effects of PLGA concentration in acetone and dexamethasone (DEX) concentration in acetone on particle size (with sodium taurocholate held constant at 0.5% (w/v)); **B**. Effects of dexamethasone concentration in acetone and the aqueous concentration of sodium taurocholate (ST, % w/v) on nanoparticle zeta potential (ζ, with PLGA concentration in acetone held constant at 20 mg/mL); **C**. Effects of PLGA and dexamethasone concentrations in acetone on encapsulation efficiency (EE, with sodium taurocholate held constant at 0.5% (w/v)). P-values for the statistically significant effects of the parameters were as follows: [PLGA] on particle size, <0.0001; [ST] on ζ, 0.0015; [DEX] on EE, 0.0032; $[DEX]^2$ on EE, 0.0182; $[PLGA]^2$ on EE, 0.0203. These plots were generated by using Statgraphics Plus 5.1 software (SAS Inc., Minneapolis, MN).

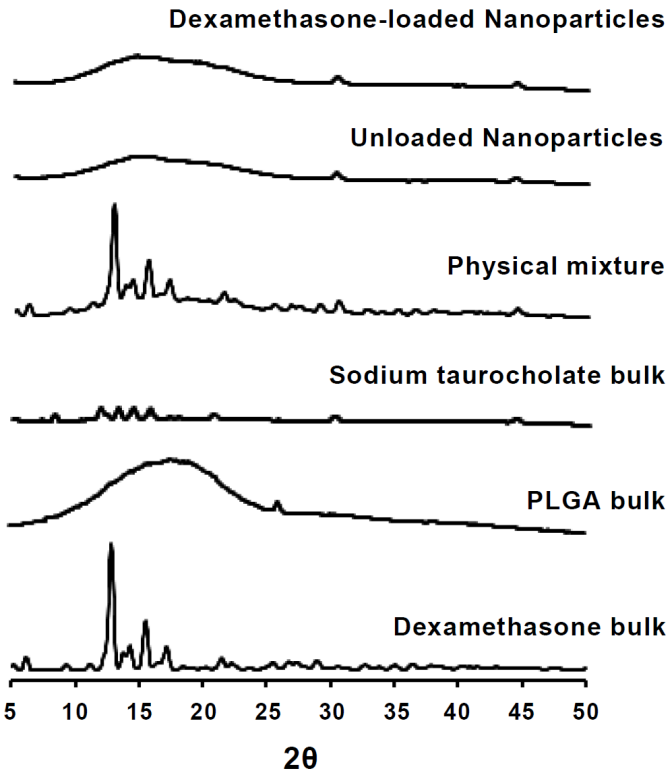

Figure 2.
Powder X-ray diffraction patterns of the following samples (bottom to top): bulk dexamethasone, bulk PLGA, bulk sodium taurocholate, a physical mixture of the aforementioned samples, unloaded PLGA nanoparticles (without dexamethasone, but prepared in the presence of sodium taurocholate), and dexamethasone-loaded PLGA nanoparticles. Curves were displaced along the ordinate for better visualization.

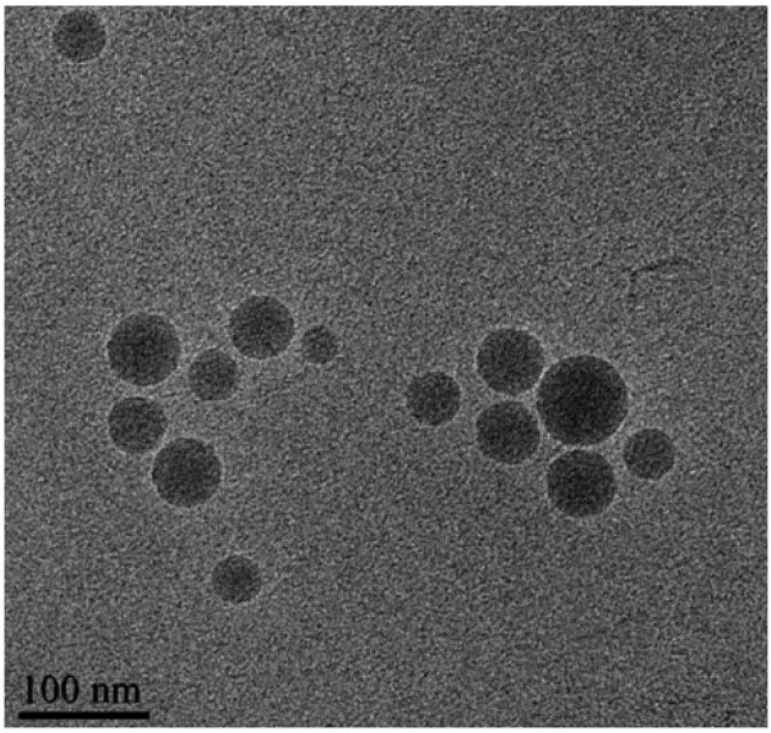

Figure 3.
A representative cryo-TEM image of dexamethasone-loaded nanoparticles (Formulation #1 in Table 1).

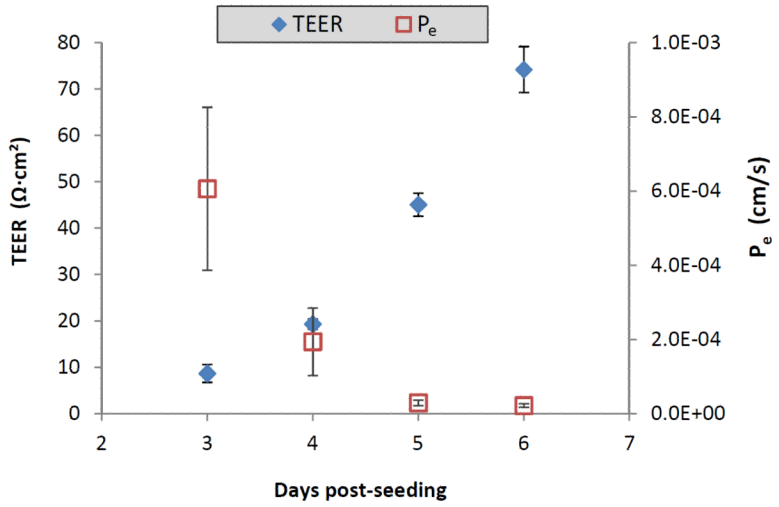

Figure 4.

Comparison of transepithelial electrical resistance (TEER) of BeWo b30 cell monolayers and the apparent permeability (P_e) of Lucifer yellow across the cell monolayers on days 3-6 post-seeding. P_e was calculated at the two-hour time point as described in the text; data are presented as the average ± standard deviation (n=4).

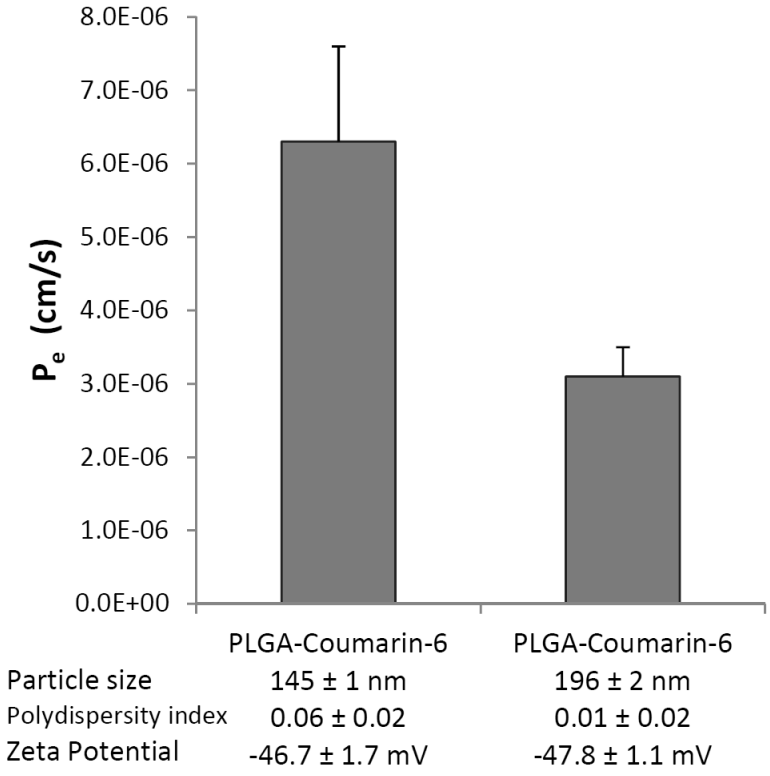

Figure 5.

Influence of particle size on the apparent permeability (P_e) of PLGA-nanoparticles across BeWo b30 cell monolayers. These nanoparticles did not contain dexamethasone, but were loaded with the fluorescent compound coumarin-6; these nanoparticles were prepared in water (without sodium taurocholate). The 145-nm particles were prepared with 20 mg/mL PLGA in acetone, and the 196-nm particles were prepared with 40 mg/mL PLGA. Initial nanoparticle concentrations applied to the apical (maternal) chamber matched those applied for the experiments from the first formulation in Table 4. The transport medium (DMEM) was without phenol red. P_e was calculated at the two-hour time point as described in the text; data are presented as the average ± standard deviation (n=3).

Table 1

Experimental runs and the observed responses for the full factorial design. Results are expressed as mean ± standard deviation (n=3).

Independent formulation variables				Dependent responses			
Formulation	**[Dexamethasone] in acetone (mg/mL, X_1)**	**[PLGA] in acetone (mg/mL, X_2)**	**[Sodium taurocholate] in the aqueous phase (%, X_3)**	**Particle size (nm, Y_1)**	**PDI (Y_2)**	**Zeta potential (mV, Y_3)**	**Encapsulation efficiency (%, Y_4)**
1	1	20	0.5	146 ± 2	0.08 ± 0.07	−64.3 ± 1.3	60.1 ± 0.8
2	2	20	0.5	144 ± 2	0.04 ± 0.04	−59.5 ± 3.4	56.4 ± 0.0
3	4	20	0.5	147 ± 0	0.01 ± 0.00	−64.5 ± 2.3	88.6 ± 0.1
4	1	40	0.5	232 ± 1	0.08 ± 0.02	−63.1 ± 1.1	61.4 ± 0.2
5	2	40	0.5	223 ± 3	0.38 ± 0.28	−64.7 ± 4.6	59.3 ± 0.0
6	4	40	0.5	226 ± 4	0.22 ± 0.29	−66.3 ± 2.0	87.3 ± 0.0
7	1	60	0.5	256 ± 4	0.65 ± 0.04	−65.6 ± 0.9	69.9 ± 0.1
8	2	60	0.5	298 ± 3	0.14 ± 0.02	−66.0 ± 1.1	61.4 ± 0.2
9	4	60	0.5	268 ± 1	0.09 ± 0.03	−64.7 ± 2.2	85.3 ± 0.1
10	1	20	1.0	144 ± 2	0.20 ± 0.04	−70.1 ± 1.2	62.5 ± 0.0
11	2	20	1.0	140 ± 5	0.27 ± 0.04	−68.1 ± 0.5	72.5 ± 0.0
12	4	20	1.0	144 ± 2	0.22 ± 0.00	−67.0 ± 1.4	89.0 ± 0.0
13	1	40	1.0	186 ± 1	0.07 ± 0.03	−68.9 ± 0.4	53.9 ± 1.5
14	2	40	1.0	187 ± 3	0.27 ± 0.16	−68.0 ± 1.0	51.8 ± 0.2
15	4	40	1.0	191 ± 2	0.09 ± 0.01	−66.9 ± 1.9	74.5 ± 0.0
16	1	60	1.0	231 ± 0	0.11 ± 0.01	−66.1 ± 2.5	76.9 ± 0.1
17	2	60	1.0	264 ± 3	0.10 ± 0.03	−67.2 ± 2.3	71.3 ± 0.1
18	4	60	1.0	298 ± 8	0.60 ± 0.35	−68.3 ± 1.2	85.4 ± 0.1

Table 2

Influence of nanoformulation on the apparent permeability (P_e) of dexamethasone across BeWo b30 cell monolayers. For both formulations, the initial nominal concentration of dexamethasone added to the apical (maternal) chamber was 50 μg/mL. P_e was calculated at the two-hour time point as described in the text; data are presented as the average ± standard deviation (n=4).

Formulation	[PLGA][c]	Particle size (nm)	P_e (cm/s)
Dexamethasone alone, dissolved in DMEM[a]	N/A[d]	N/A	$4.4 \times 10^{-6} \pm 1.4 \times 10^{-6}$
Dexamethasone-loaded nanoparticles[b]	20 mg/mL	143	$4.6 \times 10^{-5} \pm 8.9 \times 10^{-6}$

[a] Dexamethasone alone (not as a nanoparticle formulation) dissolved in the transport medium (DMEM).

[b] These nanoparticles were prepared in water (without sodium taurocholate). This formulation does not appear in Table 1; the Z-average particle size for this nanoformulation was 143 ± 1 nm, the polydispersity index was 0.04 ± 0.01, and the zeta potential was −54.5 ± 0.1 mV (n=3).

[c] Concentration of PLGA in acetone during nanoparticle preparation.

[d] Not applicable.

Table 3

Influence of the sodium taurocholate concentration employed in nanoparticle preparation on the apparent permeability (P_e) of dexamethasone across BeWo b30 cell monolayers. For all formulations, the initial nominal concentration of dexamethasone added to the apical (maternal) chamber was 50 μg/mL. P_e was calculated at the two-hour time point as described in the text; data are presented as the average ± standard deviation (n=4).

Formulation	[PLGA][e]	[Sodium Taurocholate][g]	Particle size (nm)	P_e (cm/s)
Dexamethasone alone[a]	N/A[f]	0.5%	N/A	$2.5 \times 10^{-5} \pm 8.4 \times 10^{-6}$
Dexamethasone-loaded nanoparticles[b]	20 mg/mL	0.0%	143	$4.6 \times 10^{-5} \pm 8.9 \times 10^{-6}$
Dexamethasone-loaded nanoparticles[c]	20 mg/mL	0.5%	146	$6.0 \times 10^{-5} \pm 1.6 \times 10^{-5}$
Dexamethasone-loaded nanoparticles[d]	20 mg/mL	1.0%	144	$1.8 \times 10^{-4} \pm 1.0 \times 10^{-4}$

[a] Dexamethasone alone (not as a nanoparticle formulation) dissolved initially in 0.5% sodium taurocholate as a control for the nanosuspensions prepared in the presence of sodium taurocholate.

[b] This formulation appeared in Table 2, but it is presented again in this table for comparison.

[c] This is the same as Formulation #1 in Table 1.

[d] This is the same as Formulation #10 in Table 1.

[e] Concentration of PLGA in acetone during nanoparticle preparation.

[f] Not applicable.

[g] Concentration of sodium taurocholate (w/v) in the aqueous phase during nanoparticle preparation.

Table 4

Influence of particle size on the apparent permeability (P_e) of dexamethasone across BeWo b30 cell monolayers. For both formulations, the initial nominal concentration of dexamethasone added to the apical (maternal) chamber was 50 μg/mL. P_e was calculated at the two-hour time point as described in the text; data are presented as the average ± standard deviation (n=4).

Formulation	[PLGA][c]	[Sodium Taurocholate][d]	Particle size (nm)	P_e (cm/s)
Dexamethasone-loaded nanoparticles[a]	20 mg/mL	0.5%	146	$6.0 \times 10^{-5} \pm 1.6 \times 10^{-5}$
Dexamethasone-loaded nanoparticles[b]	40 mg/mL	0.5%	232	$4.8 \times 10^{-5} \pm 1.6 \times 10^{-5}$

[a] This is the same as Formulation #1 in Table 1. This formulation appeared in Table 3, but it is bpresented again in this table for comparison.

[b] This is the same as Formulation #4 in Table 1.

[c] Concentration of PLGA in acetone during nanoparticle preparation.

[d] Concentration of sodium taurocholate (w/v) in the aqueous phase during nanoparticle preparation.